Progress In Electromagnetics Research C, Vol. 85, 129–140, 2018

Study of Unequally-Excited Random Antenna Arrays for Beam Shaping

Giovanni Buonanno* **and Raffaele Solimene**

Abstract—Random arrays have been typically studied by considering real uniform excitations. This is suited for single-beam radiation patterns but does not allow for more sophisticated patterns. Indeed, only even patterns, with respect to the steering angle, can be achieved. To overcome this limitation, we recently proposed a new model whereby the excitation coefficients are not uniform and are determined by means of two random variable transformations. In this paper, we deal more extensively with the properties of this model, highlighting things that have not been pointed out previously. In order to get analytical results, we just consider symmetric random arrays. For such a case, we determine the design error, that is the cumulative distribution function of the supremum of the the difference between the actual and desired array factors. It is shown that general shaped beams can be actually achieved but at the cost of an increase of the design error as compared to the single-beam case. Numerical analysis validates the presented theory.

1. INTRODUCTION

In random array antennas radiators are arranged non-uniformly according to a probabilistic law. As well known, random arrays offer remarkable advantages, compared to the more common uniform arrays, in terms of number of required elements, occurrence of grating-lobes and frequency bandwidth. These advantages, actually, become particularly evident and predictable for a large number of radiators. Accordingly, random arrays become attractive for large apertures [1, 2].

Usually, random arrays are considered equally-excited with at most a linear phase-shift in order to steer the main-beam. This allows optimisation of the working point of the T/R module as all elements are fed at the same power level. Moreover, the nonuniform element arrangement allows control of the side-lobe level without the need to taper the excitations. However, uniform excitations are suited only for even beam-like radiation patterns. In order to achieve more complex patterns, one must address nonuniform excitations. The first study concerning unequally-excited random arrays is Steinberg's [2]. In his work, he considered both the radiators' positions and the corresponding *real* excitations being modelled as independent and identically distributed (i.i.d.) random variables. However, no clues about how the excitations are linked to the desired radiation pattern were provided, and unfortunately that scheme proved to be no better than the usual uniform excitations [1]. Indeed, the average array factor was simply scaled by the average of the current coefficients, and moreover, the variance of the array factor was higher. Similar considerations hold true for the scheme presented in [3], where the spacings between adjacent radiators, instead of the element positions, were considered as random.

In this paper, we introduce a different scheme for unequally-excited random arrays where we model the magnitude and the phase of the excitation currents by suitable transformations of the random variable describing the radiators' positions. In particular, such transformations are chosen so as to shape the radiation pattern according to the design requirements. We remark that we already exploited

Received 29 May 2018, Accepted 25 June 2018, Scheduled 12 July 2018
* Corresponding author: Giovanni Buonanno (giovanni.buonanno@unicampania.it).
The authors are with the Department of Engineering, University of Campania, Aversa, Italy.

this same philosophy for multi-beam array factors [4]. Here, we study what extent we can apply such an approach to the case of more complex array factors.

It is clear that the described scheme implicitly subtends a sort of synthesis procedure and a metric for measuring the mismatch between the reference pattern and the obtained one (the design error). To accomplish such a task here we adopt the following procedure [4]: first, the array parameters are designed so that the mean array factor is equal to the desired one; then the design error is estimated by computing how much the actual radiation pattern deviates (statistically) from such a mean. Note that the latter question is equivalent to finding the probability distribution of the magnitude maximum of a central random process. To cope with this point, different approaches have been proposed in the literature. However, they return relatively easy (though approximate) analytical formulas under some restrictive assumptions (i.e., radiation pattern weak stationarity) that in general do not hold. Here, in order to compute the design error, the up-crossing theory [5] is used. In particular, we gain advantage by restricting the study on symmetric (in the sense explained later on) random arrays. This actually allows to find a more accurate analytical estimation for the design error which does not require the aforesaid assumptions.

It is shown that there are different ways of setting the probability law to assign the radiators' positions and to choose the transformations to obtain the required excitation coefficients. Among them, random phase only excitations suffice to get the desired mean array factor. Accordingly, amplitude tapering is not necessary, and hence the advantage concerning the working point of the T/R modules is preserved. However, even though a general beam shaping can be achieved, the design error increases as compared to the single-beam case. In this framework, the number of elements plays a fundamental role since the larger such a number is, the lower the design error is. Instead, having fixed the number of radiators the performance degrades as the array aperture increases. However, the effect of the number of elements prevails, and hence random arrays for beam-shaping become convenient for large radiating array antennas.

The study is organised as in [6], considering only symmetric arrays. This is because the math is much easier, and after all there is no significant degradation in terms of the achievable performance with respect to the asymmetric case [7]. Note that herein symmetric arrays rely upon geometric arguments but also on some conditions pertaining the random variable transformations. This point will be clarified in the subsequent sections. First, the mean and variance of the array factor are calculated. Subsequently, the error function (over the *visible* angles), i.e., the distribution of the supremum of the difference between the actual and desired array factors, is pursued. Once the supremum distribution is known, the achievable performance can be statistically foreseen. The theoretical findings are finally checked through an extensive numerical analysis. In particular, the cases where the array factor must resemble a non-centred-sector, and a cosecant behavior is considered. However, before proceeding along this plan, in the next section we will recall the basics concerning random arrays which are required to make the paper self-contained.

2. UNEQUALLY-EXCITED SYMMETRIC RANDOM ARRAYS

In this section we introduce the model for unequally-excited symmetric random arrays by generalising the one concerning equal excitations studied in [7].

Consider N isotropic radiators randomly deployed within the interval $[-L/2, L/2]$ of the X axis, where $L = \tilde{L}/\lambda$ is the normalised array extent, that is the array physical aperture normalised to the wavelength λ. The number of radiators, N, is chosen even since it entails a slightly simpler mathematical notation. However, the case of an odd N can be addressed as well, as shown in [7]. The random array is assumed symmetric in the following sense. For each element located at $X_n \in [0, L/2]$ there is another one located at $-X_n$. Moreover, said I_n the excitation coefficient for the radiator in X_n, we further assume that $I_{-n} = I_n^*$, where $()^*$ stands for conjugation. Accordingly, on assuming that the mutual coupling is negligible [8], the normalised array factor can be written as [4]

$$F(u) = \frac{2}{N} \sum_{n=1}^{N/2} M(X_n) \cos[2\pi X_n u + \alpha(X_n)] \tag{1}$$

where $\theta \in [0, \pi]$ is the angle (with respect to the X-axis) of the observation direction (see Fig. 1), and $u = \cos\theta$ ranges within the *visible space* $[-1, 1]$. Moreover, the excitation coefficients have been expressed in terms of their magnitudes and phases, which is $I_n = M(X_n)\, e^{j\alpha(X_n)}$, and the conjugated relationship assumed above has been exploited. The radiator positions X_n are i.i.d. random variables which are supported (because of the symmetry assumption) over half the array aperture. Accordingly, $f(X)$ denotes the common (to all radiators) probability distribution function (pdf) of the positions. Clearly, it is supported over the interval $[0, L/2]$. It is important to note that, as opposed to the Steinberg's approach, the excitation coefficients have been expressed by the real $M(X)$ and $\alpha(X)$ transformations of the random positions. The advantage of this choice compared to the Steinberg's approach will appear shortly in this section. In particular, here, because of the symmetry assumption, $M(X)$ is an even function and $\alpha(X)$ an odd one.

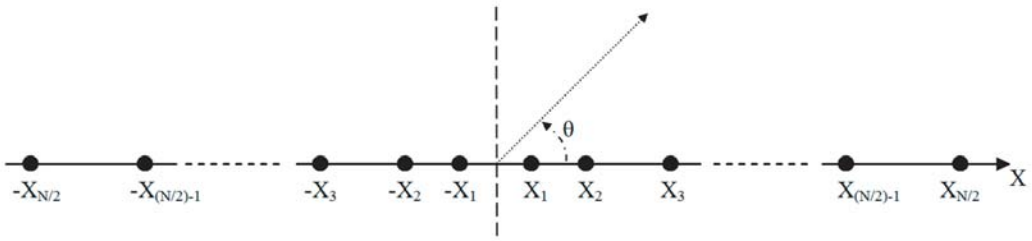

Figure 1. Geometry of a generic symmetric random arrays where the element positions are implicitly ordered.

The array factor in Equation (1) is clearly a stochastic process. As such it can be (even though partially) characterised in terms of the mean and variance. The latter can be explicitly written as [4]

$$\phi(u) = \int_0^{L/2} f(X)\, M(X) \cos[2\pi X u + \alpha(X)]\, dX \tag{2}$$

and

$$\sigma^2(u) = \frac{E[M^2(X)] + E[M^2(X)\cos(4\pi X u + 2\alpha(X))] - 2\phi^2(u)}{N} \tag{3}$$

For a large number of radiators (indeed for large $N/2$), as it is common in the framework of random arrays, the Central Limit Theorem can be invoked, and the array factor, for a given u, can be considered Gaussian distributed with the mean and variance given by Equations (2) and (3), that is $F(u) \sim \mathcal{N}[\phi(u), \sigma^2(u)]$. Moreover, for the multivariate form of the Central Limit Theorem [9], the array factor can be seen as a Gaussian process.

Let us now turn to discuss our choice concerning the excitation coefficients. In Steinberg's approach the excitations are still random but are assumed independent on the radiators' positions X_n. As shown in [2], this actually does not lead to any advantage with respect to the equally-excited case. Indeed, the mean array factor is only scaled in amplitude, by means of a constant coefficient (by the average of the excitation coefficients), and the shape of $\phi(u)$ is only due to $f(X)$. The latter, being a real function, allows to achieve only even array factors. Instead, by the model in Equation (2), the excitation functions directly enter the $\phi(u)$ expression. Therefore, $M(X)$ and $\alpha(x)$ provide further degrees of freedom that can be exploited to shape $\phi(u)$, which in turn no longer needs to be an even function.

Let us now turn to address how the random array can be generated (including the excitation coefficients) in order to satisfy the design requirement. According to the previous discussion, once N and L have been fixed, it amounts to setting $f(x)$, $M(X)$ and $\alpha(X)$ according to desired array factor. To this end, the following steps can be carried out:

(i) Choosing the desired array factor, $\tilde{\phi}_{DES}(u)$. Note that according to Equation (2) $\tilde{\phi}_{DES}(u)$ must be a real function.

(ii) Determining the equivalent *continuous* current $i(X)$ supported on the array aperture that yields

$\tilde{\phi}_{DES}(u)$. This is achieved by a standard Fourier procedure, that is

$$i(X) = \begin{cases} \int_{-\infty}^{\infty} \tilde{\phi}_{DES}(u)\, e^{-j2\pi Xu}\, du & 0 \le X \le L/2 \\ 0 & \text{elsewhere} \end{cases} \tag{4}$$

Note that since $\tilde{\phi}_{DES}(u)$ is real, $i(X)$ is Hermitian, hence it is sufficient to compute it over half the array aperture. Moreover, $i(X)$ in Equation (4) actually corresponds to the (actual) desired array factor

$$\phi_{DES}(u) = \int_{L/2}^{L/2} i(X) e^{j2\pi Xu} dX \tag{5}$$

which is indeed the least mean square error approximation of $\tilde{\phi}_{DES}(u)$, when the latter is not a band-limited function.

(iii) Setting $f(X)M(X) = 2|i(X)|$ and $\alpha(X) = \angle i(X)$. At this juncture, while the sough after phase function $\alpha(X)$ is uniquely determined, different choices are indeed possible for $f(X)$ and $M(X)$. This is because choosing $\phi_{DES}(u)$ only fixes their product. However, whatever strategies one may want to adopt for setting $f(X)$ and $M(X)$, it must hold that $\int_0^{L/2} f(X)\, dX = 1$, since $f(X)$ is a pdf.

In order to introduce the strategies for setting $M(X)$ and $f(X)$ that are used in the following, we need to elaborate more in depth on item (iii). According to the previous discussion, once $|i(x)|$ has been determined, an easy way to proceed is to choose $M(x)$ and hence to find $f(X)$ or vice versa. This leads to the following three different approaches.

(i) The amplitude excitation function is fixed according to some assigned law, that is $M(X) = \gamma\tilde{M}(X)$, and hence it results in $f(X) = 2|i(X)|/\gamma\tilde{M}(X)$. Here, the constant must be defined as $\gamma = \int_0^{L/2} 2|i(X)|/\tilde{M}(X)dX$ which assures that $f(X)$ is actually a pdf. Choosing $\tilde{M}(X) \neq 0\ \forall\ X$ assures the feasibility of this approach.

(ii) The amplitude excitation function is set constant, that is, $M(X) = M$, consequently $f(X) = 2|i(X)|/M$. Since $\int_0^{L/2} f(X)\, dX = 1$, we are not free to choose such a constant at will. It must be fixed as $M = \int_0^{L/2} 2|i(X)|dX$ so as to actually have $f(X)$ as representative of a pdf. Note that this approach coincides with the previous one when $\tilde{M}(X)$ is set uniform. Therefore, this approach is a particular case of the method 1. For convenience, we keep them separate. Also note that in this case, the excitation coefficients turn out to be pure complex phase terms, and therefore the advantage concerning the working point of the T/R modules is restored.

(iii) The pdf $f(X)$ is fixed, and consequently the amplitude excitation function is determined by $M(X) = 2|i(X)|/f(X)$. This strategy is basically the opposite of the previous one. It offers the possibility of being free to choose standard pdf for $f(X)$ that facilitates the generation of the random element positions X_n.

All the approaches presented above set the parameters of the unequally excited random arrays that enable obtaining the mean radiation pattern equal (in the mean square sense) to the desired one. However, they lead to different design errors. This can be appreciated by Eq. (3) that returns the corresponding variance functions. The latter allows for a comparison of different design schemes and gives important clues concerning the achievable performance. However, in order to estimate the design error we need a metric that more specifically measures how close the random array factor is to the desired one. This point will be addressed in the next section.

3. DESIGN ERROR ESTIMATION

Assume that we have fixed the random array parameters as described above. Then, we have $\phi(u) = \phi_{DES}(u)$. Accordingly, the design error is related to the stochastic process $\epsilon(u) = F(u) - \phi_{DES}(u)$. Hence, $\epsilon(u)$ is a Gaussian centered stochastic process, that is $\epsilon(u) \sim \mathcal{N}[0, \sigma^2(u)]$, where $\sigma^2(u)$ is the

same as in Eq. (3). Note that in $\epsilon(u)$ we considered $\phi_{DES}(u)$ instead of $\tilde{\phi}_{DES}(u)$. This is of course because $\phi_{DES}(u)$ is the best one that can aim for finite array apertures. Moreover, since random arrays are better suited for large array apertures, as we pointed out in the introduction, it can be reasonably considered that $\tilde{\phi}_{DES}(u) \simeq \phi_{DES}(u)$.

A first easy way to characterise the design error is to determine the interval within which $\epsilon(u)$ can range. In our case, this is equivalent to studying the p-per-cent level curves $r_p(u)$, that is

$$P\{|\epsilon(u)| \leq \gamma\,\sigma(u)\} = P\{-\gamma\,\sigma(u) \leq \epsilon(u) \leq \gamma\,\sigma(u)\} = p\,\% \tag{6}$$

where we have set $r_p(u) = \gamma\,\sigma(u)$. Of course, the real constant γ is related to the value of the probability $p\%$. For example, because of the Gaussian distribution of $\epsilon(u)$, $\gamma = 3$ yields $p\% = 0.997$. In general, the link between γ and p is more involved, since [7]

$$p\% = Q(-\gamma) - Q(\gamma) \tag{7}$$

with $Q(t) = (1/\sqrt{2\pi}) \int_t^\infty e^{-y^2/2}\,dy$. Therefore, in general, in order to find the link between γ and p, one needs to resort to the tabulated version of $Q(\cdot)$ or to invoke some approximation of it and solve the corresponding non-linear polynomial equation [10].

The p-per-cent level curves allow identifying the strip $[-r_p(u), r_p(u)]$ within which the error $\epsilon(u)$ belongs with probability p. This is, however, a fairly *punctual* characterisation in the sense that it varies with u. In order to get a more complete characterisation we employ the uniform norm distribution of $|\epsilon(u)|$, that is [6]

$$\begin{aligned} P\left\{\varepsilon = \max_{u\in[-1,1]} |\epsilon(u)| \leq \xi\right\} &= P\{|\epsilon(u)| \leq \xi\ \forall\ u \in [-1,1]\} \\ &= P\{-\xi \leq \epsilon(u) \leq \xi\ \forall\ u \in [-1,1]\} \end{aligned} \tag{8}$$

In particular, to estimate Eq. (8), we employ the up-crossing approach. In detail, say ξ the level with respect to which the number of up-crossings has to be estimated and say N_ξ the random variable that counts how many times $|\epsilon(u)|$ up-crosses ξ (i.e., crosses ξ with a positive slope). Accordingly, $P\left\{\varepsilon = \max_{u\in[-1,1]} |\epsilon(u)| \leq \xi\right\}$ coincides with the probability that $N_\xi = 0$ or, equivalently, with $1 - P(\mathcal{N}_\xi \geq 1)$. Since, by Markov inequality

$$P(\mathcal{N}_\xi \geq 1) \leq E[\mathcal{N}_\xi] \tag{9}$$

the problem can be conveniently cast as the determination of $E[\mathcal{N}_\xi]$. To this end, the famous Rice's formula can be exploited [5, 11], once it is adapted to the symmetric array case at hand [7]. In fact, since $\epsilon(u)$ is a real random process, determining the up-crossings of $|\epsilon(u)|$ is actually equivalent to the two barrier problem where one has to study the up-crosses of $\epsilon(u)$ and $\tilde{\epsilon}(u) = -\epsilon(u)$ for the given level $\xi > 0$. Since $\epsilon(u)$ and $\epsilon'(u) = d\epsilon(u)/du$, and of course $\tilde{\epsilon}(u)$ and $\tilde{\epsilon}'(u) = d\tilde{\epsilon}(u)/du$, are jointly Gaussian, the mean number of up-crossings can be written as [7]

$$E\{\mathcal{N}_\xi\} = 2\int_{-1}^{1} du \int_0^\infty \epsilon'\, \frac{e^{-\frac{1}{2[1-\rho^2(u)]}\left\{\frac{\xi^2}{\sigma^2(u)} - 2\rho(u)\frac{\xi\epsilon'}{\sigma(u)\sigma'(u)} + \frac{\epsilon'^2}{\sigma'^2(u)}\right\}}}{2\pi\sigma(u)\sigma'(u)\sqrt{1-\rho^2(u)}} d\epsilon' \tag{10}$$

where $\sigma'^2(u)$ is the variance of $\epsilon'(u)$, and $\rho(u) = E[\epsilon(u), \epsilon'(u)]/(\sigma(u)\sigma'(u))$ is the correlation coefficient that can be computed as shown in [7]. It must be remarked that Eq. (9) is meaningful only when $E[\mathcal{N}_\xi] \leq 1$. More in general, $E\left[\mathcal{N}_\xi\right]$ can be used to get a direct estimation of $P\{\varepsilon \leq \xi\}$, under, however, a further assumption that up-crossing points occur as a random point Poisson process [12]. In this case, it can be shown that [6]

$$P\{\varepsilon \leq \xi\} \approx \left\{Q\left[-\frac{\xi}{\sigma(-1)}\right] - Q\left[\frac{\xi}{\sigma(-1)}\right]\right\} e^{-E[\mathcal{N}_\xi]} \tag{11}$$

and eventually, the latter is the estimation of the ε distribution that will be used in the sequel.

4. NUMERICAL ANALYSIS

In this section, we conduct a numerical critical analysis in order to asses to what extent the proposed random array schemes are able to shape the array factor and the related design error. In particular, we selected two types of array factors for $\tilde{\phi}_{DES}(u)$: the sector and the cosecant patterns. These are more complex than the relatively simple multi-beams addressed in [4] and are often employed in literature as reference for the introduction of continuous source and uniformly-spaced unequally-excited arrays synthesis methods [13, 14].

Let us start by the sector-pattern case. In this case, we set the *initial* desired array factor equal to

$$\tilde{\phi}_{DES}(u) = \begin{cases} 0 & -1 \le u < 0.3 \\ 1 & 0.3 \le u < 0.7 \\ 0 & 0.7 \le u \le 1 \end{cases} \iff \tilde{\phi}_{DES}(\theta) = \begin{cases} 0 & 72.54^\circ \le \theta \le 180^\circ \\ 1 & 45.57^\circ \le \theta < 72.54^\circ \\ 0 & 0^\circ \le \theta < 45.57^\circ \end{cases} \tag{12}$$

where it is reminded that $\theta = \cos^{-1}(u)$ is the observation angle. From Eq. (4) the equivalent continuous current can be determined in closed form as

$$i(X) = \begin{cases} 0.4\, e^{-j\pi X}\, \mathrm{sinc}(0.4X) & 0 \le X \le L/2 \\ 0 & \text{elsewhere} \end{cases} \tag{13}$$

where $\mathrm{sinc}(X) = \sin(\pi X)/(\pi X)$. Accordingly, the mean array factor is $\phi(u)$ by setting $f(X)M(X) = 0.8|\mathrm{sinc}(0.4X)|$ and $\alpha(X) = -\pi X + \angle\{\mathrm{sinc}(0.4X)\}$. Now, the next step is to determine the behaviors of $f(X)$ and $M(X)$. According to the methods presented previously, besides the case $M(X) = M$ (method 2) we set:

- for method 1, $\tilde{M}(X) = \{7 \times 10^{-3}[1 - (4/L)\, X] + (8/L^2)\, X\}$ (raised triangular $M(X)$ case) and $\tilde{M}(X) = \{5.6 \times 10^{-3}/\sin[5.6 \times 10^{-3}(L/2)]\} \cos(5.6 \times 10^{-3} X)$ (raised cosine $M(X)$ case);
- for method 3 $f(X) = 2/L$ (uniform pdf case), $f(X) = \{7 \times 10^{-3}[1 - (4/L)\, X] + (8/L^2)\, X\}$ (raised triangular pdf case) and $f(X) = \{[5.6 \times 10^{-3}/\sin(5.6 \times 10^{-3}(L/2))] \cos(5.6 \times 10^{-3} X)\}$ (raised cosine pdf case).

The variance behaviors for the considered six cases are shown in Fig. 2 with $N = 200$ and $L = 500$. As can be seen, the strategy of setting $M(X)$ returns better results than setting $f(X)$. In particular, the constant $M(X)$ (method 2) is the best one while the worst case occurs for the uniform pdf. Accordingly, we choose the constant $M(X)$ method for the rest of the analysis. In Fig. 3, we analyse the variance behavior for such a strategy for different values of the number of radiators and array lengths. In

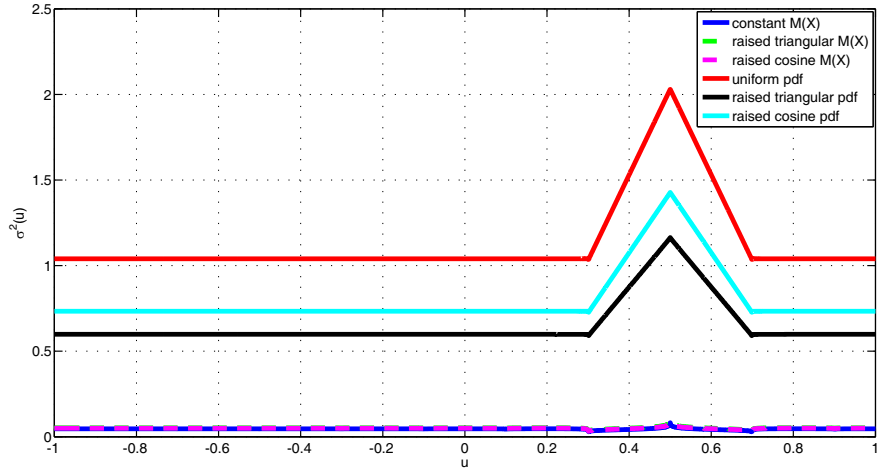

Figure 2. Behaviour of the array factor variance for different choices of $f(X)$ and $M(X)$ for the sector beampattern case. The number of the antenna elements is $N = 200$ and the aperture is $L = 500$.

particular, it can be recognised that, for fixed N, the variance increases with the array length, whereas for a fixed length it decreases by increasing N. This is consistent with Eq. (3). Furthermore, even when the average spacing between the radiators remains constant, the variance does not follow the same behavior. This can be clearly seen by comparing the cases $(N = 200, L = 200)$ and $(N = 500, L = 500)$ or $(N = 200, L = 100)$ and $(N = 500, L = 1000)$. However, the number of antenna elements plays a major role compared to the array aperture and dominates the variance behavior.

In Fig. 4, we turn to show some sample array factors and the related $\phi(u)$ for the same cases as in Fig. 3. As can be expected, the array factors exhibit the classical oscillating behavior of a random process. Nonetheless, they follow the desired pattern by oscillating around it. Also, it is seen that the samples deviate from $\phi(u)$ according to the variance behavior sketched in the previous figure. For

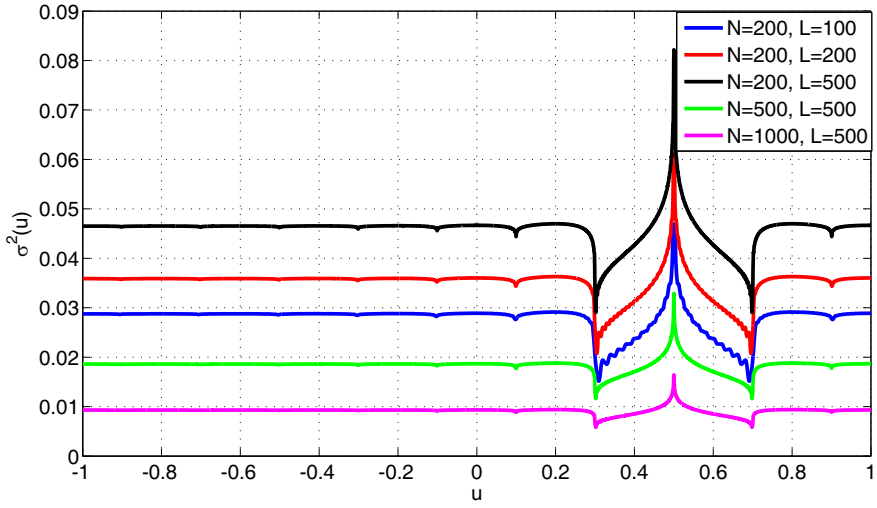

Figure 3. Behaviour of the array factor variance for different values of the number of antenna elements and array aperture in the case of the sector beampattern. The function $M(X)$ is chosen constant.

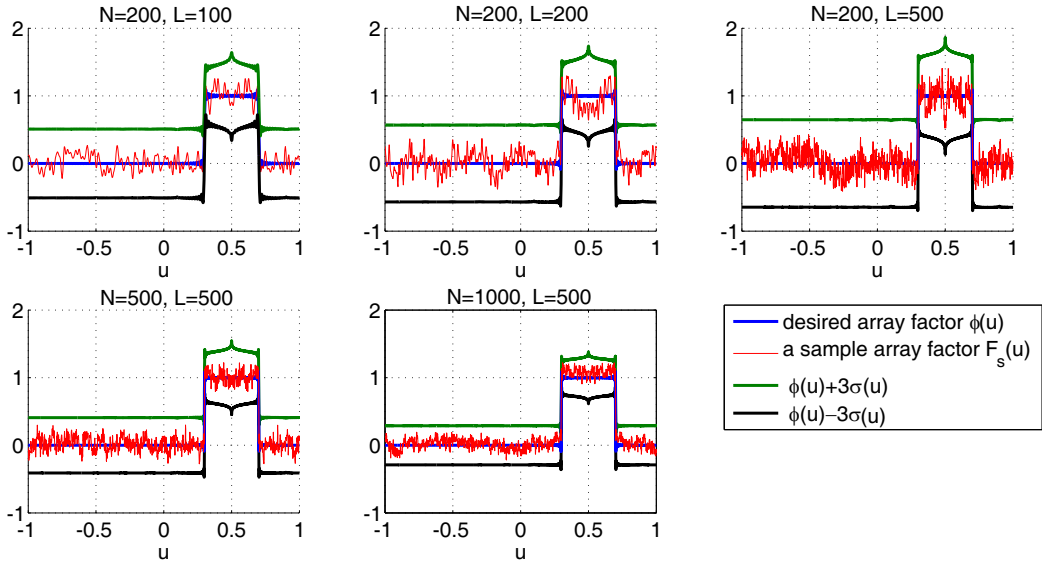

Figure 4. Behaviours of the desired and a sample array factors for different values of the number of antenna elements and array aperture for the sector-pattern case. The function $M(X)$ is chosen constant. The green and black solid lines show $\tilde{\phi}_{DES}(u) + r_p(u)$ and $\tilde{\phi}_{DES}(u) - r_p(u)$, respectively, with $p = 99.7$.

example, it is seen that for $N = 200$ the sample array factor deviates less when the aperture is shorter. Again, for $N = 1000$ and $L = 500$ the sample array factor is "closer" to the desired array factor than for $N = 200$ and $L = 100$, or when $N = 500$ and $L = 500$ with respect to $N = 200$ and $L = 200$. In the same figure $\tilde{\phi}_{DES}(u) + r_p(u)$ and $\tilde{\phi}_{DES}(u) - r_p(u)$, with $p = 99.7$, are reported as well. As can be seen, they may provide a too severe estimation of the design error.

Finally, the empirical and theoretical ε distributions are reported in Fig. 5. It is seen that the theoretical estimation works very well. Basically, these curves confirm the trend described above; however they allow for an estimation of the maximum design error according to the parameters of the random array.

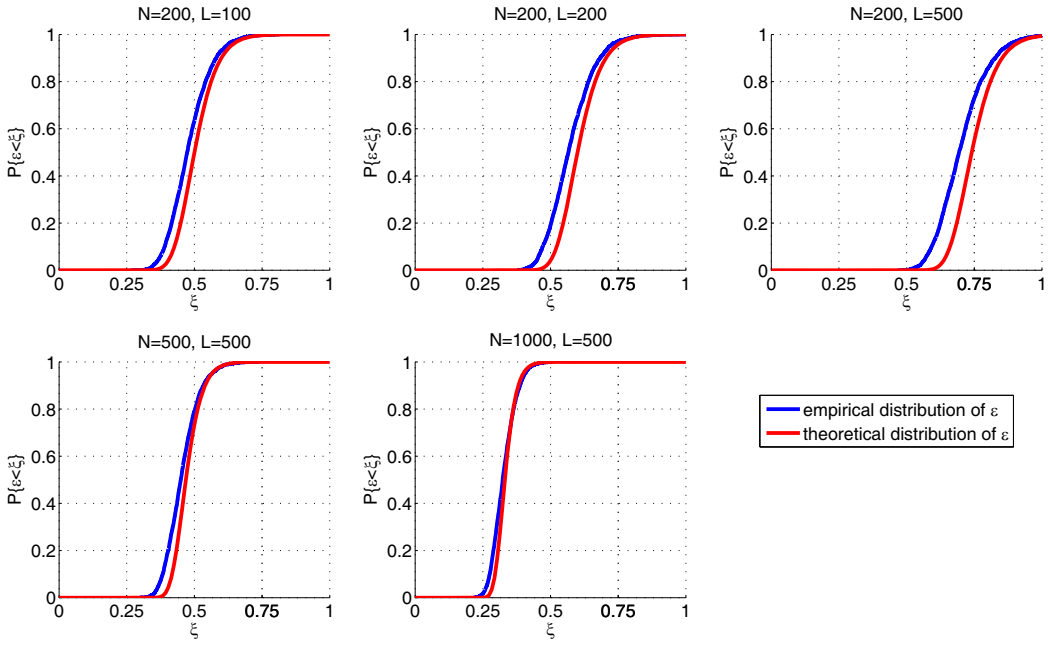

Figure 5. Behaviour of the empirical and theoretical distributions of ε for the sector-pattern case, when the number of antenna elements and the array aperture vary.

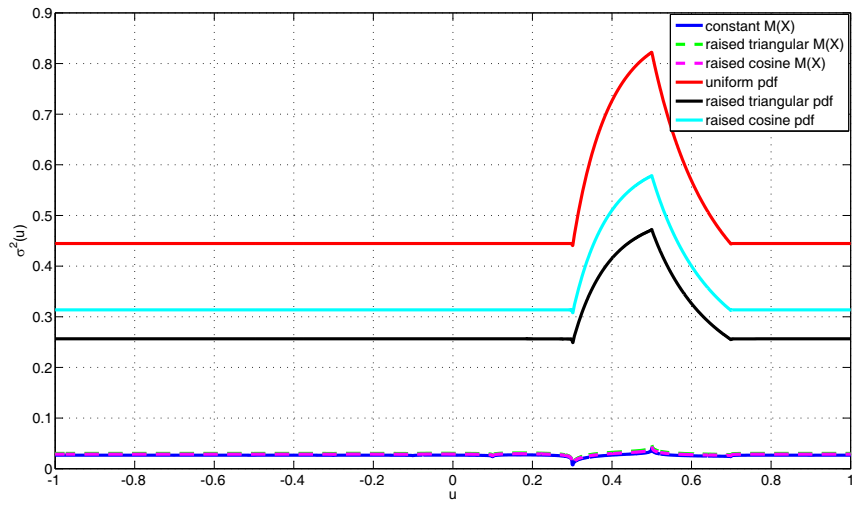

Figure 6. Behaviour of the array factor variance for different choice of $f(X)$ and $M(X)$ for the cosecant beampattern case. The number of the antenna elements is $N = 200$ and the aperture is $L = 500$.

We now switch to consider the cosecant-pattern case. In this case, the desired array factor is given by

$$\tilde{\phi}_{DES}(u) = \begin{cases} 0 & -1 \le u < 0.3 \\ \dfrac{0.3}{u} & 0.3 \le u < 0.7 \\ 0 & 0.7 \le u \le 1 \end{cases} \iff \tilde{\phi}_{DES}(\theta) = \begin{cases} 0 & 72.54^\circ \le \theta \le 180^\circ \\ \dfrac{0.3}{\cos\theta} & 45.57^\circ \le \theta < 72.54^\circ \\ 0 & 0^\circ \le \theta < 45.57^\circ \end{cases} \tag{14}$$

and the same analysis as the previous one is then achieved. Fig. 6 shows the comparison of the variances for $N = 200$ and $L = 500$ for the considered six cases. Once again it can be deduced that setting $M(X)$ and then getting $f(X)$ is better than doing the opposite. Moreover, the case of $M(X)$ constant is still the best one. Fig. 7 shows the bahaviors of the variances of the array factor related to the cases in which

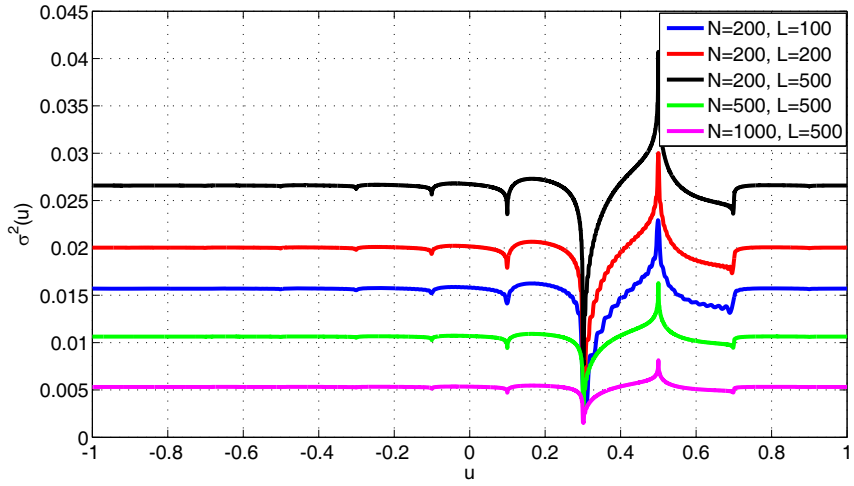

Figure 7. Behaviour of the array factor variance for different values of the number of antenna elements and array aperture for the cosecant-pattern. The function $M(X)$ is chosen constant.

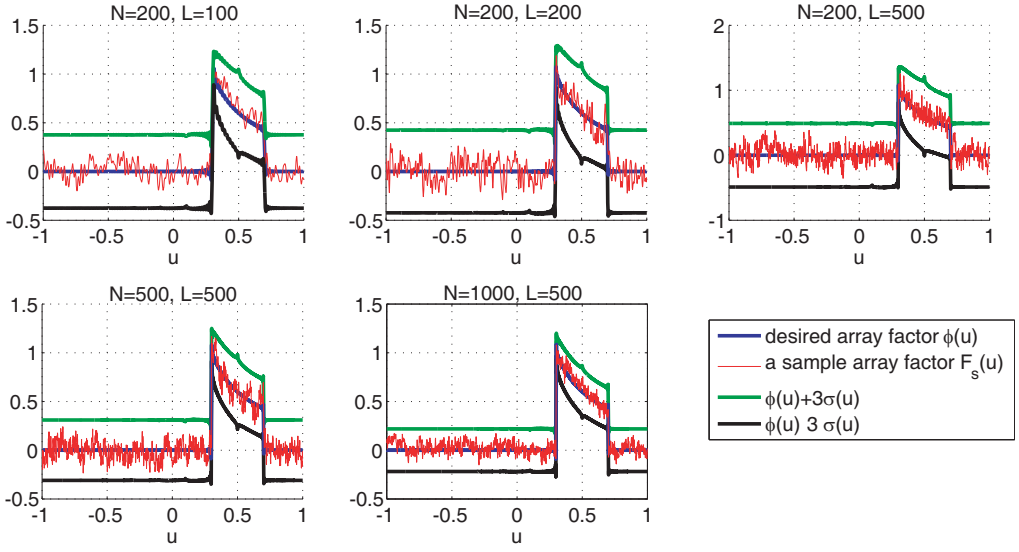

Figure 8. Behaviours of the desired and a sample array factors for different values of the number of antenna elements and array aperture for the cosecant-pattern case. The function $M(X)$ is chosen constant. The green and black solid lines show $\tilde{\phi}_{DES}(u) + r_p(u)$ and $\tilde{\phi}_{DES}(u) - r_p(u)$, respectively, with $p = 99.7$.

the transformation $M(X)$ is constant, and the parameters N and L vary. It can be noted again that, for fixed N, the variance increases with the extension of the array aperture while if this extension is fixed then it decreases when N becomes higher. Looking at Fig. 8, even in the cosecant case one can conclude that the samples of the array factor oscillate around the mean array factor, $\phi(u)$, and obviously, these oscillations become smaller and smaller as the number of radiators increases (having fixed the array aperture). Furthermore, observing also the curves $\tilde{\phi}_{DES}(u) + r_p(u)$ and $\tilde{\phi}_{DES}(u) - r_p(u)$ with $p = 99.7$ reported in the same figure, it can still be recognised that these curves may be too pessimistic. Finally, in Fig. 9 the empirical and theoretical ε distributions are shown. It can be noted that the theoretical estimation is very much closer to the experimental ones. Eventually, for the cosecant pattern case the same conclusions as for the sector case can be drawn out.

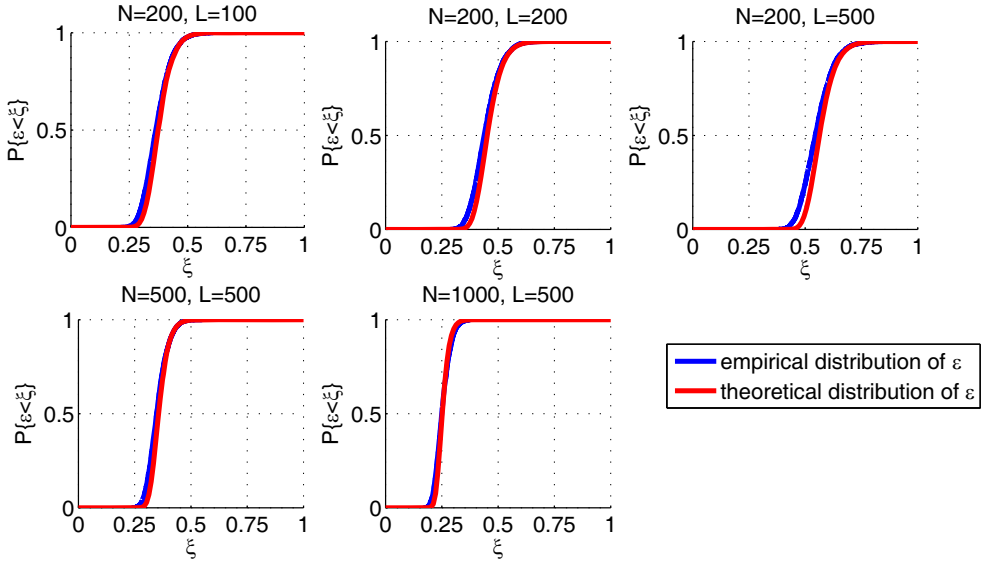

Figure 9. Behaviour of the empirical and theoretical distributions of ε for the cosecant-pattern case, when the number of antenna elements and the array aperture vary.

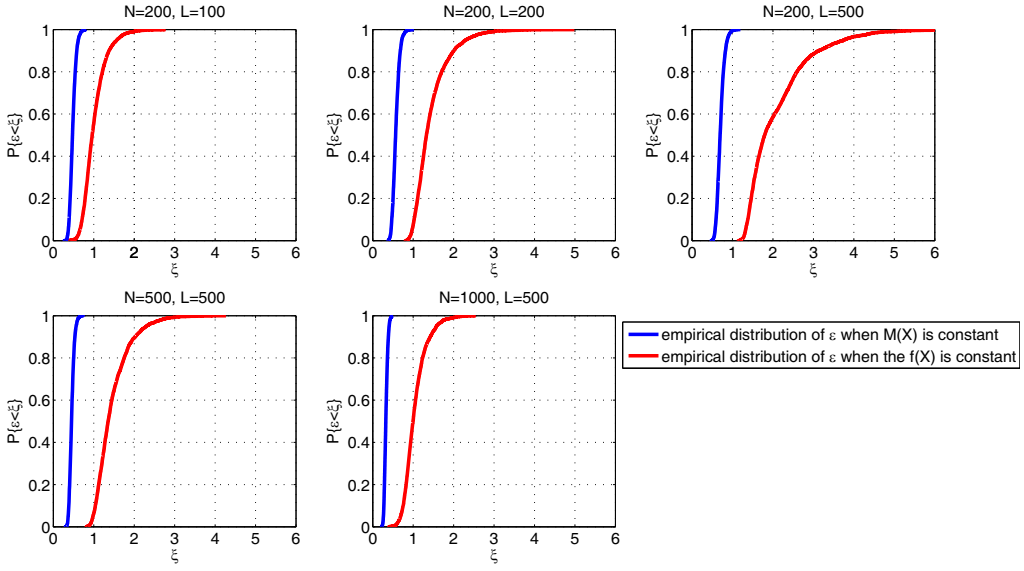

Figure 10. Comparison between the empirical distribution of ε for the sector-pattern case, for the cases $M(X)$ is constant and $f(X)$ is uniform, respectively.

We just end this section by turning to the question of the best choice for setting $M(X)$ and $f(X)$. Previously, according to the variance behavior, we have argued that method 2 is the best one. It is worth checking if it is actually so by inspecting the design error cumulative distribution (i.e., the ε-distributions). This is achieved in Figs. 10 and 11, respectively for the two considered cases. These figures actually confirm that method 2 always allows for a lower design error.

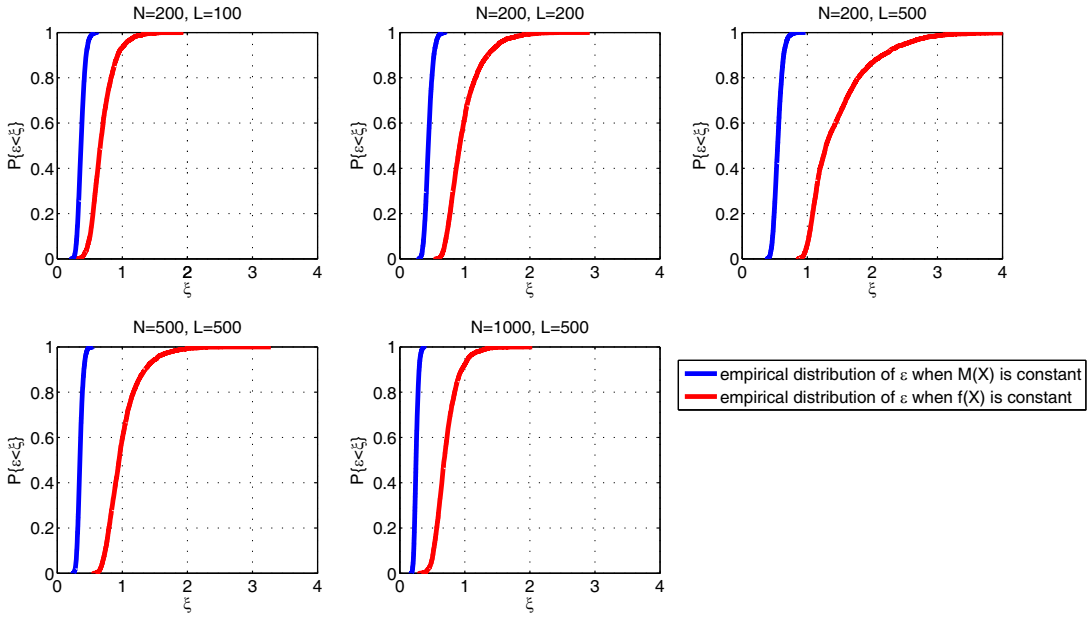

Figure 11. Comparison between the empirical distribution of ε for the cosecant-pattern case, for the cases $M(X)$ is constant and $f(X)$ is uniform, respectively.

5. CONCLUSION

In this paper we want to verify some properties of the above model that in [4] have not been taken into consideration. In particular, here the dominant theme is the modality of choice of the function related to the excitation coefficient magnitudes and to the radiators pdf, which in [4] had less weight. From our analysis, it has been found that the best choice is the one in which the excitations are pure exponentials. We have in fact observed that lower levels of the variance of the array factor are obtained when the random variable transformation, associated with excitation magnitudes, is constant. In addition, we have also investigated the effect that the array aperture has on performance, showing that when the number of antenna elements is fixed, the larger the aperture is, the higher the variance levels are. Conversely, when the array aperture is fixed, the higher the number of radiators, the more the sample array factors approach the desired one. This finding was also verified through the centered array factor distributions. Since the advantage of constantly choosing the function $M(X)$ was made by evaluating the variance of the array factor, we wanted to verify this also by resorting to the centered array factor distributions, in particular comparing this case with that in which the radiators positions pdf is uniform. As expected, the choice made at the beginning was confirmed to be the best.

In every way, although the numerical results presented are only partial, it can be said that when the number of antenna elements is very high (for example $N = 5000$) as in the case of radar arrays [15], the presented model can be useful for a probabilistic synthesis of unequally-excited aperiodic arrays.

ACKNOWLEDGMENT

The authors kindly thank Giuseppina Nuzzo for proofreading the manuscript.

REFERENCES

1. Lo, Y. T., "A mathematical theory of antenna arrays with randomly spaced elements," *IEEE Transactions on Antennas and Propagation*, Vol. 12, 257–268, 1964.
2. Steinberg, B. D., *Principles of Aperture and Arrays System Design*, Wiley, New York, 1976.
3. Queiroz, W. J. L. and M. S. Alencar, "Project of antenna arrays with random parameters," *Proc. Brazilian Microwave and Optoelectronics Society/Microwave Theory and Techniques Society Int. Microwave and Optoelectronics Conf.*, 33–38, 2003.
4. Buonanno, G. and R. Solimene, "Unequally-excited linear totally random antenna arrays for multi-beam patterns," *IET Microwaves Antennas & Propagation*, 2018, http://digital-library.theiet.org/content/journals/10.1049/iet-map.2017.1206.
5. Donvito M. B. and S. A. Kassam, "Characterization of the random array peak sidelobe," *IEEE Transactions on Antennas and Propagation*, Vol. 27, 379–385, 1979.
6. Buonanno, G. and R. Solimene, "Generalised random binned antenna arrays," *Progress In Electromagnetics Research C*, Vol. 78, 129–143, 2017.
7. Buonanno, G. and R. Solimene "Large linear random symmetric arrays," *Progress In Electromagnetics Research M*, Vol. 52, 67–77, 2016.
8. Lo, Y. T., "Aperiodic arrays," *Antenna Handbook, Vol. 2, Antenna Theory*, Y. T. Lo and S. W. Lee (eds.), Chap. 14, Chapman and Hall, 1993.
9. Feller, W., *An Introduction to Probability Theory and its Applications, Volume II*, Wiley, New York, 1966.
10. Couch, L. W., *Digital and Analog Communication Systems*, 8th edition, Prentice Hall, One Lake Street, Upper Saddle River, New Jersey, 2013.
11. Cramér, H. and M. R. Leadbetter, *Stationary and Related Stochastic Processes: Sample Function Properties and their Applications*, Dover Publications, New York, 2004.
12. Krishnamurthy, S., D. Bliss, and V. Tarokh, "Sidelobe level distribution computation for antenna arrays with arbitrary element distribution," *2011 Conference Record of the Forthy Fifth Asilomar Conference on Signals, System and Computers (ASILOMAR)*, 2045–2050, Nov. 2011.
13. Chakraborty, A., B. N. Das, and S. S. Gitindra, "Determination of phase functions for a desired one-dimensional pattern," *IEEE Transaction on Antennas and Propagation*, Vol. 29, 502–506, 1981.
14. Srinivasa Raju, G. R. L. V. N., B. N. Das, and G. S. N. Raju, "Synthesis of cosecant and square patterns for EMC applications," *IOSR Journal of Electronics and Communications Engineering (IOSR-JECE)*, Vol. 9, 1–6, 2014.
15. Fourikis, N., *Advanced Array Systems, Applications and RF Technologies*, Academic Press, 2000.